BNL-NUREG-61620

Practical Application of Equivalent Linearization Approaches to Nonlinear Piping Systems*

Young J. Park
Department of Advanced Technology
Brookhaven National Laboratory
Upton, New York 11973

Charles H. Hofmayer
Department of Advanced Technology
Brookhaven National Laboratory
Upton, New York 11973

ABSTRACT

The use of mechanical energy absorbers as an alternative to conventional hydraulic and mechanical snubbers for piping supports has attracted a wide interest among researchers and practitioners in the nuclear industry. The basic design concept of energy absorbers (EA) is to dissipate the vibration energy of piping systems through nonlinear hysteretic actions of EA's under design seismic loads. Therefore, some type of nonlinear analysis needs to be performed in the seismic design of piping systems with EA supports.

The equivalent linearization approach (ELA) can be a practical analysis tool for this purpose, particularly when the response spectrum approach (RSA) is also incorporated in the analysis formulations. In this paper, the following ELA/RSA methods are presented and compared to each other regarding their practicality and numerical accuracy:

- Response spectrum approach using the square root of sum of squares (SRSS) approximation (denoted RS in this paper).
- Classical ELA based on modal combinations and linear random vibration theory (denoted CELA in this paper).
- Stochastic ELA based on direct solution of response covariance matrix (denoted SELA in this paper).

New algorithms to convert response spectra to the equivalent power spectral density (PSD) functions are presented for both the above CELA and SELA methods. The numerical accuracy of the three ELA/RSA's are studied through a parametric error analysis. Finally, the practicality of the presented analysis methods is demonstrated in two application examples for piping systems with EA supports.

*This work was performed under the auspices of the U.S. Nuclear Regulatory Commission.

DISCLAIMER

Portions of this document may be illegible in electronic image products. Images are produced from the best available original document.

Practical Application of Equivalent Linearization Approaches to Nonlinear Piping Systems

Young J. Park
Department of Advanced Technology
Brookhaven National Laboratory
Upton, New York 11973

Charles H. Hofmayer
Department of Advanced Technology
Brookhaven National Laboratory
Upton, New York 11973

INTRODUCTION

The use of mechanical energy absorbers as an alternative to conventional hydraulic and mechanical snubbers for piping supports has attracted a wide interest among researchers and practitioners in the nuclear industry (e.g., Ref. [1] and [2]). The basic design concept of energy absorbers (EA) is to dissipate the vibration energy of piping systems through nonlinear hysteretic actions of EA's under design seismic loads. Therefore, some type of nonlinear analysis needs to be performed in the seismic design of piping systems with EA supports.

The equivalent linearization approach (ELA) can be a practical analysis tool for this purpose, particularly when the response spectrum approach (RSA) is also incorporated in the analysis formulations. In this paper, the following ELA/RSA methods are presented and compared to each other regarding their practicality and numerical accuracy:

- Response spectrum approach using the square root of sum of squares (SRSS) approximation (denoted RS in this paper).
- Classical ELA based on modal combinations and linear random vibration theory (denoted CELA in this paper).
- Stochastic ELA based on direct solution of response covariance matrix (denoted SELA in this paper).

New algorithms to convert response spectra to the equivalent power spectral density (PSD) functions are presented for both the above CELA and SELA methods. The numerical accuracy of the three ELA/RSA's are studied through a parametric error analysis. Finally, the practicality of the presented analysis methods is demonstrated in two application examples for piping systems with EA supports.

EQUIVALENT LINEARIZATION APPROACHES

RS Method. According to the classical study by Caughey (1963), the equivalent stiffness, k_{eq} of a hysteretic system is obtained based on the slowly-varying assumption on the nonlinear oscillation, as

$$K_{eq} = \frac{1}{\pi U}\int_0^{2\pi} F(u)\cdot\cos\theta\, d\theta, \quad u = U\cdot\cos\theta \qquad (1)$$

in which, U is the peak displacement amplitude; F(u) is the nonlinear restoring force for the largest hysteresis loop as a function of displacement, u.

For the equivalent modal damping, h_{eq}, the formulation proposed by Tansirikongkol and Pecknold (1980), which is a slight modification of the formulation proposed by Caughey (1963), is used in this study.

$$h_{eq,r} = h_{o,r}\frac{\omega_r}{\omega_{eq,r}} + \frac{\sum_i \epsilon_{ir}^2\cdot S_i}{2M_r\cdot\omega_{eq,r}^2} \qquad (2)$$

$h_{o,r}$ = elastic modal damping
ω_r = frequency for r-th mode
$\omega_{eq,r}$ = equivalent frequency
M_r = modal mass
ϵ_{ir} = modal strain of component-i
S_i = normalized hysteresis area of component-i

$$= \frac{A}{\pi U^2} = \frac{4}{\pi}K_o(1-\alpha)\left(\frac{\mu-1}{\mu^2}\right)\cdots$$

...for bilinear system

A = area of a hysteresis loop
μ = ductility factor of the response

The SRSS approximation is used in the iterative solution scheme, in which the above k_{eq} and h_{eq} are updated, followed by a new eigenvalue analysis of the equivalent linear system.

CELA Method. The method is based on the linear random vibration theory and a modified Kryloff-Bogoliubov equivalent linearization approach. A displacement component, u_i, in a piping system is expressed as,

$$u_i = \sum_r \phi_{ir} q_r + \sum_m \varphi_{im} X_m \qquad (3)$$

in which, q_r is the r-th normal mode response; ϕ_{ir} is the eigenvector of the fixed-based system; X_m is the differential displacement at the m-th fixed degree of freedom; and φ_{im} is the displacement mode due to the m-th differential displacement. Assuming stationality of responses, the covariance for a pair of displacements, u_i and u_j, are obtained as,

$$R_{u_i u_j}(o) = \sum_r \sum_s \phi_{ir}\phi_{is} R_{rs} + \sum_m \sum_n \varphi_{im}\varphi_{jn} \cdot \bar{R}_{mn} \qquad (4)$$

in which, R_{rs} is the covariance for the r-th and s-th normal mode responses; and $\bar{R}_{mn}$ is the covariance for the m-th and n-th differential displacements.

$$R_{rs} = \sum_k \sum_l C_{kl} \cdot \beta_{rk}\,\beta_{sl} \int_{-\infty}^{\infty} H_r(\omega) \cdot H_s(\omega)\sqrt{S_k(\omega) \cdot S_l(\omega)}\,d\omega \qquad (5)$$

$$\bar{R}_{mn} = C_{mn} \int_{-\infty}^{\infty} \frac{1}{\omega_4} \sqrt{S_m(\omega) \cdot S_n(\omega)}\; d\omega \qquad (6)$$

in which, C_{kl} is the correlation coefficient for the k-th and l-th excitations; β_{rk} is the r-th participation factor for the k-th excitation; $H_r(\omega)$ is the transfer function for the r-th mode; and $S_k(\omega)$ is the k-th PSD function.

The equivalent component stiffness, k_{eq}, and modal damping, h_{eq}, can be defined using the peak distribution functions, $p_1(u, \sigma_e)$ and $p_2(u, \sigma_e)$, as,

$$K_{eq} = \int_0^{\infty} K_{eq}(u) \cdot p_1(u, \sigma_e)\; du \qquad (7)$$

$$h_{eq} = \int_0^{\infty} h_{eq}(u) \cdot p_2(u, \sigma_e)\, du \qquad (8)$$

in which, σ_e is the standard deviation of the strain response. The foregoing eqs. (1) and (2) can be used for the peak response dependent stiffness and damping, $K_{eq}(u)$ and $h_{eq}(u)$.

For the above peak distribution functions, p_1 and p_2, various mathematical models have been suggested in the past (e.g., Refs. [5] and [6]). In this study, the peak distribution functions, p_1 and p_2, are determined in a purely empirical manner based on the observation of the past simulation studies on bilinear hysteretic systems (e.g., Ref. [5] and [7]). The details of the distribution functions are given in an Appendix to this paper.

SELA Method. The method is the direct solution of the response covariance matrix based on the stochastic equivalent linearization approach proposed by Atalik and Utku (1976). This approach may be one of the most popular research topics in this area, and has been applied to hysteretic systems with a relatively small number of degrees of freedom (e.g., Refs. [9] and [10]). According to Wen (1980), the nonlinear restoring force, q, is expressed as,

$$q = \alpha K u + (1 - \alpha) K Z \qquad (9)$$

$$\dot{Z} = f(\dot{u}, Z) \qquad (10)$$

in which u and $\dot{u}$ = the relative displacement and velocity; K = the initial stiffness; α = the postyield stiffness ratio; and Z = the hysteretic component with the unit of displacement. According to Ref. [11], the above hysteretic function, $f(\dot{u}, Z)$, for a bilinear system is expressed as,

$$\dot{Z} = \dot{u} - 0.5\dot{u}\,H_1(Z) - 0.5\,|\dot{u}|\,H_2(Z) \qquad (11)$$

where

$$H_1(Z) = U(Z - \Delta) + U(-Z - \Delta)$$
$$H_2(Z) = U(Z - \Delta) - U(-Z - \Delta) \qquad (12)$$

in which U(x) = unit step function; and Δ = the yield displacement.

Another class of hysteretic models are obtained by smoothing these functions, $H_1(Z)$ and $H_2(Z)$, as follows:

$$H_1(Z) = \frac{|Z|^n}{\Delta^n}$$
$$H_2(Z) = \frac{Z\,|Z|^{n-1}}{\Delta^n} \qquad (13)$$

and therefore

$$\dot{Z} = \dot{u} - \frac{0.5}{\Delta^n}\dot{u}\,|Z|^n - \frac{0.5}{\Delta^n}|\dot{u}\,|Z|Z|^{n-1} \qquad (14)$$

More detailed description on the practical application of this approach to nonlinear piping systems, including the determination of the maximum response statistics, can be found in Refs. [12], and [13].

RESPONSE SPECTRUM APPROACHES

RS Method. It is one of the significant advantages of this approach that the response spectra can be used directly as the excitation input. However, as the modal damping values change during the iteration according to eq. (2), an interpolation/extrapolation scheme is necessary for converting the response spectral values for an arbitrary damping value, h. In this study, the following empirical formulations are used (Ref. [14]):

$$\frac{S(h)}{S(h=0)} = \frac{1}{1+10h} \quad \text{for } 0.02<h<0.05$$
$$\frac{S(h)}{S(h=0.05)} = \frac{2.25}{1.75+10h} \quad \text{for } 0.05<h<0.2 \tag{15}$$

CELA Method. Since the method is based on linear random vibration theory, the input response spectra should be converted to an equivalent PSD function. A high accuracy direct conversion method has been developed recently for this purpose (Ref. [15]). The conversion algorithm is summarized below.

The objective here is to obtain an equivalent PSD function, $S_g(\omega)$, given a target acceleration response spectrum, $R_t(\omega, h)$, and a modulating envelope function, I(t), which can be represented by the effective duration, T_e.

The unknown PSD function is discretized at radial frequencies, ω_j, and expressed as the sum of a series of discretized power components, p_j, as,

$$S_g(\omega) = \sum_{j=1}^{m} S(\omega_j)\,\Delta\omega_j\,\delta(\omega_j) = \sum_{j=1}^{m} p_j\,\delta(\omega_j) \tag{16}$$

in which, $\delta(\omega)$ is the Dirac delta function; and $\Delta\omega_j$ is the incremental radial frequency.

Using the above discretized power components, p_j , the target response spectrum at radial frequencies, ω_k , can be approximated by a superposition of the component response spectra as,

$$R_t^2(\omega_k, h) = \sum_{j=1}^{m} p_j\,R_{k,j}^2(\omega_k, \omega_j, h), \qquad k = 1,n \tag{17}$$

in which, $R_{k,j}$ represents the peak acceleration response of an SDOF system with a vibration frequency of ω_k , and a viscous damping of h, which is excited by an extremely narrow-banded process whose PSD function is $\delta(\omega_j)$. Using the peak factor approximation by Davenport (1963), $R_{k,j}$ is determined as,

$$R_{k,j}(\omega_k, \omega_j, h) = \left\{\sqrt{2\ln(\nu_j T_e)} + \frac{3.772}{\sqrt{2\ln(\nu_j T_e)}}\right\} \cdot \sqrt{\frac{1+4h^2\chi^2}{(1-\chi^2)^2+4h^2\chi^2}} \tag{18}$$

in which, $\nu_j = \omega_j/2\pi$, and $\chi = \omega_j/\omega_k$. Given a modulating function, I(t), the equivalent duration, T_e , can be defined as,

$$T_e = \left\{\int_0^t I(t)\,dt\right\} / \max\{I(t)\} \tag{19}$$

The above power components, p_j , can be obtained by solving a standard least squares problem as,

minimize

$$\sum_{k=1}^{n}\left\{R_t^2(\omega_k,h) - \sum_{j=1}^{m} p_j\,R_{k,j}^2(\omega_k,\omega_j,h)\right\}^2 \tag{20}$$

subject to $\quad p_j \geq 0, \quad j = 1,m$

Mathematical libraries to solve the above least squares problem is widely available (e.g., IMSL programs). The equivalent PSD function is directly obtained as,

$$S(\omega_j) = p_j / \Delta\omega_j, \quad j = 1, m \tag{21}$$

The method was applied to response spectra with steep slopes and sharp turning points; one is the Reg. Guide 1.60 spectrum (Ref. [18]), and the other is a Newmark-Hall type spectrum (Ref. [19]). The following modulating function was assumed to determine the effective duration, T_e, of 16.8 sec.

$$\begin{aligned} I(t) &= (t/3)^2 && t<3 \text{ sec.} \\ &= 1.0 && 3<t<16 \text{ sec.} \\ &= e^{-3(t-16)/13} && 16<t<20 \text{ sec.} \end{aligned} \tag{22}$$

To discretize both the PSD and response spectrum functions, 100 frequency points between 0.15Hz and 50Hz, equally spaced on a logarithmic scale, were used (i.e., m = n = 100). The comparisons with the Monte Carlo simulations (500 samples) are shown in Fig. 1 and the obtained PSD functions are shown in Fig. 2. The simulations were performed by using the modulating function of eq. (22) and the PSD functions of Fig. 2. The simulation results slightly overestimate the zero-period acceleration (ZPA) values in both cases. Otherwise,

TABLE 1. CALCULATED COMPONENT PARAMETERS

COMPONENT	REG. 1.60			NEWMARK-HALL		
	f_{gj} (Hz)	h_{gj} (%)	p_j (IN^2/S^3)	f_{gj} (Hz)	h_{gj} (%)	p_j (IN^2/S^3)
1	9.4	29	1120	10.5	20	619
2	6.1	20	81	7.0	20	215
3	4.8	22	51	4.8	20	61
4	3.6	20	26	3.3	20	25
5	2.9	20	9.2	2.2	20	8.4
6	2.3	24	17.2	1.5	18	3.1
7	0.9	20	0.17	0.78	20	0.08

a close match between the target and simulated response spectra can be observed.

It may be fair to point out here that the results presented above are based on the characterization of the earthquake motions by a single damping value, which would not guarantee an equal fit to other damping values. A further study may be necessary for resolving this multiple damping issue.

SELA Method. In this analysis scheme, the input excitation can only be given by shot noise processes (Ref. [9] and [13]). The frequency characteristics of the ground motion are included by means of additional equations of motion, e.g., an additional mass-spring system inserted between the input shot-noise excitations and the structural model, such as the use of the Tajimi-Kanai spectrum. To overcome this limitation, a new analysis scheme is proposed. The method converts an arbitrary response spectrum to a PSD function which represents a linear combination of SDOF response processes (Ref. [13]).

First, consider a seismic acceleration process, $\ddot{x}_j$, which is approximated by a linear combination of mutually independent filtered shot-noise processes, x_j, i.e.,

$$x_g = \sum_{j=1}^{k} x_j \tag{23}$$

The above "component" processes, x_j, represent the displacement responses of SDOF systems subjected to mutually independent shot noise processes, $f_j(t)$.

$$\ddot{x}_j + 2h_{gj}\,\omega_{gj}\,\dot{x}_j + \omega_{gj}^2\,x_j = -f_j(t) \qquad j = 1,k \tag{24}$$

$$E[f_i(t)f_j(t)] = 2\pi p_j\, I(t) \quad \text{for} \quad i = j$$
$$= 0 \quad \text{for} \quad i \neq j \tag{25}$$

in which, h_{gj} and ω_{gj} are the component filter parameters; p_j is the component power intensity; and I(t) is the deterministic modulating function with a unit maximum value (i.e., $I_{max} = 1.0$). In the above, the displacement responses rather than the acceleration responses are used to model the input motions. This is to account for the fact that most response spectra or floor spectra possess a predominantly low-passing frequency characteristic (see Fig. 2).

The power spectrum of the approximated process, $S_{\ddot{x}}(\omega)$, is expressed as,

$$S_{\ddot{x}}(\omega) = \sum_{j=1}^{k} p_j S_j(\omega) \tag{26}$$

where

$$S_j(\omega) = \frac{1}{(\omega^2 - \omega_{gj}^2)^2 + 4h_{gj}^2\omega_{gj}^2\omega^2} \tag{27}$$

Therefore, the corresponding acceleration response spectrum, $\bar{R}_{\ddot{x}}(\omega_0, h_0)$, for the approximated process is expressed by the following relationship:

$$\bar{R}^2_{\ddot{x}}(\omega_0,h_0) = \sum_{j=1}^{k} p_j R_j^2(\omega_0,h_0) \tag{28}$$

The component power intensities, p_j, are obtained by following the same procedure given in eq. (20), while the filter parameters, $\omega_{g\,j}$ and $h_{g\,j}$, are determined through a sensitivity analysis on the calculated numerical error defined by eq. (20). Therefore, an iterative procedure is necessary to obtain the optimal filter parameters.

The foregoing response spectra were used as application examples. The calculated component power intensities and the filter parameters are tabulated in Table 1, and obtained response spectra and PSD functions are given in Figs. 3 and 4. Since only seven (7) components were used for these examples, the calculated PSD functions are not as smooth as the ones in Fig. 2.

TABLE 2. MAJOR CAUSES OF NUMERICAL ERRORS IN ELA

TYPE OF ELA	CAUSE OF NUMERICAL ERROR
All ELA's	• Inability to reproduce "drift" response due to accumulation of plastic deformation.
RS	• Under/Overshooting detuning effects. • Over estimation of equivalent damping. • Interpolation/Extrapolation of response spectral values to account for damping changes. • SRSS approximation.
CELA	• Conversion from response spectra to PSD functions. • Selection of peak distribution functions to determine k_e and h_e.
SELA	• Error in RSA. • Gaussian assumption on nonlinear response statistics (particularly hysteretic components). • Evaluation of maximum response statistics.

ERROR ANALYSIS

ELA's are subjected to various forms of numerical errors; some are due to the intrinsic deficiencies in the ELA itself, and others are attributed to the unique approximation schemes adopted in an analysis approach. Both qualitative and quantitative evaluations of numerical errors associated with ELA's are necessary for a successful application to practical engineering problems. Table 2 lists major causes of numerical errors that have been identified in the past numerous studies in this area.

The error due to "drifting", or the accumulation of permanent plastic deformation, is one of the most serious numerical errors that is associated with any form of an ELA. However, a past simulation study (Ref. [11]) indicates that this error can be negligible when the postyield stiffness ratio, α (ratio of the postyield stiffness to the initial stiffness), is higher than 0.04 to 0.05, regardless of the other factors such as the level of nonlinearity and the type of hysteretic models.

It is beyond the scope of this paper to single out and quantitatively evaluate each of the items listed in Table 2. Rather, the combined numerical errors associated with the three ELA's are evaluated under structural and loading conditions which can be encountered in a typical seismic analysis.

A simple SDOF system with a bilinear or a smoothed model of eq. (14) (n = 1) is used. The viscous damping is assumed to be 5% and the postyield stiffness ratio is chosen to be 0.05. The foregoing Newmark-Hall type response spectrum is used as the seismic excitation model. As illustrated in Fig. 5, three initial vibration frequencies, 1Hz, 7Hz and 20Hz, are considered. Due to the detuning in the nonlinear responses, the system may move into the peak (20Hz), stay on the top of the peak (7Hz), or move away from the peak (1Hz). For both the CELA and SELA analyses, the foregoing equivalent response spectrum model of Figs. 1(b) and 3(b) are used without any modifications.

The calculated response results are compared with Monte Carlo simulations (MCS), in which the equivalent PSD function in Fig. 2(b) was used to generate 500 samples of acceleration time histories.

The calculated results are summarized in Figs. 6(a) through 6(d), in which the abscisa represents the normalized excitation amplitude (ratio of zero-period acceleration to the yield strength of the SDOF system) and the ordinate represents the calculated peak ductility factor, μ_{max}.

The results for the RS approach indicate that the method tends to underestimate the responses up to a ductility factor of 3 to 4 in all the cases. For the case of f = 7Hz, in which the system stays on the top of the flat spectral peak, the analysis tends to overshoot at the higher nonlinear response range as indicated in Figs. 6(b) and 6(c).

The results from the CELA method slightly underestimate or overestimate the simulation results depending on the relative position of the vibration frequency to the spectral peak. Up to a ductility factor of 6 to 8, the observed numerical errors are not significant in comparison with other methods.

The response results by the SELA method, on the other hand, are unsatisfactory. In all the cases the analysis underestimates the peak response values, particularly for higher frequency cases (see Fig. 6(a)). This probably is attributed to the deficiency in the mathematical model to calculate the maximum response statistics. It should be noted that the numerical errors in the evaluation of variance responses are not significant in the presented cases since the error due to the Gaussian assumption is already accounted for using an error correction scheme from Ref. [11], and the error due to drifting is negligible when the postyield stiffness ratio is higher than 0.04 to 0.05. A further study is necessary to improve the accuracy in estimating the maximum response statistics for the SELA method. Currently, there exist no widely acceptable mathematical models for this purpose.

Among the items in Table 2, the numerical error due to the SRSS approximation in the RS approach is not accounted for in the above error analysis. This is discussed in the following application examples.

APPLICATION EXAMPLES

As examples of the practical application of the ELA's to nonlinear piping systems, two piping systems supported by EA's, as illustrated in Figs. 7 and 8, were analyzed. The outside diameter and wall thickness of the main pipes are 216.3mm and 10.3mm for the Feedwater (F)-line, and 267.4mm and 12.7mm for the Main Steam (M)-line, respectively. These piping systems are the scaled models (scale factor is about 1/2.5) of actual piping in PWR and BWR nuclear power plants, and will be tested using Nuclear Power Engineering Corporation's (NUPEC) large shaking table at Tadotsu

TABLE 3. EQUIVALENT FREQUENCIES AND DAMPING OF M-LINE

MODE	ELASTIC MODEL		RS		CELA	
	Frequency (Hz)	Damping (%)	Frequency (Hz)	Damping (%)	Frequency (Hz)	Damping (%)
1	7.95	2.5	6.32	20.5	6.10	17.7
2	9.65	2.5	7.93	13.9	8.33	7.4
3	11.5	2.5	9.67	11.3	9.98	5.4
4	13.6	2.5	10.7	22.6	11.9	11.3
5	15.4	2.5	11.9	4.1	14.4	3.0

TABLE 4. EQUIVALENT FREQUENCIES AND DAMPING OF F-LINE

MODE	ELASTIC MODEL		RS		CELA	
	Frequency (Hz)	Damping (%)	Frequency (Hz)	Damping (%)	Frequency (Hz)	Damping (%)
1	13.2	2.5	9.43	21.4	9.73	16.5
2	13.9	2.5	11.6	11.5	11.8	7.1
3	17.4	2.5	15.1	8.8	15.6	5.5
4	21.1	2.5	19.4	5.3	19.7	4.3
5	23.6	2.5	22.8	3.3	23.1	2.9

TABLE 5. COMPARISON OF PEAK RESPONSES OF M-LINE

ITEMS	LOCATION	NTH	RS	CELA
Disp. u_x(mm)	Node-150	5.42	5.46	5.64
Accel. A_x (g)	Node-150	3.09	5.64	2.89
EA Deform. (mm)	LED-2	4.98	4.52	4.69
Pipe Stress (kg/mm^2)	Elm.-(3)	3.33	2.42	3.49

TABLE 6. COMPARISON OF PEAK RESPONSES OF F-LINE

ITEMS	LOCATION	NTH	RS	CELA
Disp. u_x(mm)	Node-330	6.11	5.65	5.91
Accel. A_x (g)	Node-330	2.83	3.36	2.79
EA Deform (mm)	EAB-2	6.90	4.68	6.05
Pipe Stress (kg/mm^2)	Elm.-(1)	2.46	2.16	2.25

Engineering Laboratory in Shikoku, Japan.

The piping systems are subjected to horizontal (in the x-direction) and vertical (in the z-direction) acceleration motions as illustrated in Fig. 9, which are the calculated floor responses of a PWR nuclear power plant. The response spectra and the PSD function for the horizontal component are shown in Figs. 10 and 11. The PSD function in Fig. 11 represents an equivalent stationary process with an effective duration, T_e. The effective duration was defined by the time interval in which the power of the accelerogram attains 5% and 95% of the total power. The amplitude of the PSD functions were adjusted to reproduce the peak acceleration values, which were estimated using the Gumbel's type-I distribution function.

In this paper, the foregoing RS approach (based on SRSS approximation) and CELA method (based on linear random vibration theory) are used to compare with conventional nonlinear time history analyses. The application of the SELA method (based on stochastic equivalent linearization) is not attempted herein mainly because the size of the response covariance matrices are excessively large (approximately 1300 x 1300) for these finite element models. In applying the CELA method, the equivalent PSD function in Fig. 11 was directly used (effective duration is 15.7 sec.). In modeling the piping systems, straight and circular curved beam elements were used for the pipes, and axial springs with the smoothed hysteretic model (eq. 14 with n=2) were used to model three EA's for each piping system (i.e., EAB-1, 2, 3 for the F-line an LED-1, 2, 3 for the M-line).

First, a conventional nonlinear time history (NTH) analysis was performed for both the piping systems. An example of the calculated responses of the EA supports is given in Fig. 12. Then, the foregoing RS and CELA analyses were performed; in the analyses, the eigenvalue solutions were updated four (4) times, assuming a cutoff frequency of 50 Hz (i.e., 13 modes for the M-line and 16 modes for F-line were used in the analyses).

The calculated equivalent vibration frequencies and damping for the first 5 modes are tabulated in Tables 3 and 4. A few calculated response results are also compared in Tables 5 and 6. In general, the response results by both the RS and CELA methods correlate reasonably well with the time history analysis results, although the CELA method gives a better agreement than the RS method. Based on a more detailed evaluation of the calculated response results, the SRSS approximation used in the RS method is considered to be a major cause of the observed differences between the RS and CELA analyses.

An example of an acceleration transfer function is shown in Fig. 13 for the F-line. This transfer function was calculated using the CELA method as a ratio of PSD functions.

$$|H(\omega)|^2 = S_R(\omega)/S_g(\omega) \qquad (29)$$

in which, $S_R(\omega)$ and $S_g(\omega)$ are the response and input acceleration PSD functions. There is a significant broad-banded peak at around 10 Hz in the transfer function of Fig. 13. This reflects not only the higher damping values for the lower modes (see Table 4), but also the fact that the first two modes are "merged" into one combined mode.

SUMMARY AND CONCLUSIONS

Three types of equivalent linearization approaches were presented and compared to each other regarding their practicality and numerical accuracy. For a practical application, all the methods were formulated into the response spectrum approach. Two types of conversion schemes were presented to obtain the equivalent PSD functions which were consistent with the prescribed response spectra. The application examples to nonlinear piping systems with energy absorbing supports indicate that the RS method (based on the SRSS approximation) and the CELA method (based on linear random vibration theory) are practical analysis tools for evaluating the seismic response of complex nonlinear piping system with reasonable accuracy. A comparison with the conventional time history analysis results indicates that the CELA method, after some improvements on the definitions of the equivalent component stiffness and the modal damping values, gives a better correlation than the RS method.

ACKNOWLEDGEMENT

The work presented in this paper was performed under the auspices of the U.S. Nuclear Regulatory Commission as a part of a collaborative effort between the USNRC and the Ministry of International Trade and Industry (MITI) of Japan. The authors wish to thank Dr. N. Chokshi for his support and encouragement during the course of this study. The authors also wish to thank N.Tanaka and H.Abe of NUPEC, as well as many other members of the NUPEC, and Mitsubishi and Hitachi staff for providing the information on the piping systems, as well as the permission to use them as numerical examples. Thanks are also due to Prof. Kohei Suzuki of Tokyo Metropolitan University for his detailed review comments.

NOTE

The findings and opinions expressed in this paper are those of the authors, and do not necessarily reflect the views of the U.S. Nuclear Regulatory Commission or Brookhaven National Laboratory.

REFERENCES

[1] Fujita, K., et al., "Study on a Rotary Type Lead Extrusion Damper as a High Damping Support for Nuclear Piping Systems," SMiRT 11, Vol. K, Tokyo, Japan, 1991, pp. 475-479.

[2] Shibata, H., et al., "Development of the Elastic-Plastic Damper and its Application to the Piping System in Nuclear Power Plants," SmiRT 11, Vol. K, Tokyo, Japan, 1991, pp. 487-492.

[3] Caughey, T.K., "Equivalent Linearization Techniques," Journal of the Acoustical Society of America, Vol. 35, Num. 11, November 1963, pp. 1706-1711.

[4] Tansirikongkol, V. and Pecknold, D.A., "Approximate Modal Analysis of Bilinear MDF Systems," Journal of Engineering Division, ASCE, Vol. 106, No. EM2, April 1980, pp. 361-375.

[5] Lutes, L.D., "Stationary Random Response of Bilinear Hysteretic Systems, " Ph.D. Thesis, California Institute of Technology, 1967.

[6] Soda, S. and Tani, S., "Basic Study on Statistical Aseismic Design of Tall Building," Transactions of Architectural Institute of Japan, No. 288, Feb. 1980, pp. 97-105.

[7] Chokshi, N.C. and Lutes, L.D., "Maximum Response Statistics for Yielding Oscillator," Journal of Engineering Mechanics Division, ASCE, Vol. 102, No. EM6, Dec. 1976, pp. 983-996.

[8] Atalik, T.S. and Utku, S., "Stochastic Linearization of Multi-Degree-Of-Freedom Nonlinear Systems," Earthquake Eng. Struct. Dyn., Vol. 4, 1976, pp. 411-420.

[9] Wen, Y.K., "Equivalent Linearization Hysteretic Systems Under Random Excitation," Journal of Applied Mechanics, Vol. 47, No. 1,1980, pp. 150-154.

[10] Park, Y.J., Wen, Y.K., and Ang., A.H-S., "Random Vibration of Hysteretic Systems Under Bi-directional Ground Motions," Earthquake Engineering and Structural Dynamics, Vol. 14, 1986, pp. 543-557.

[11] Park, Y.J., "Equivalent Linearization for Seismic Responses, Part I: Formulation and Error Analysis," Journal of engineering Mechanics, ASCE, Vol. 118, No. 11, Nov. 1992, pp. 2207-2226.

[12] Park, Y.J. and Reich, M., "Nonlinear 3D Piping Analysis Under Stochastic Dynamic Loads," Nuclear Engineering and Design, Vol. 126, 1991, pp. 233-243.

[13] Park, Y.J., "Nonlinear 3-D Piping Analysis Under Stochastic Dynamic Loads: Response Spectrum Approach, " ASME/PVP Conference, Vol. 237-1, New Orleans, June 1992, pp. 217-222.

[14] "Ultimate Strength and Deformation Capacity of Buildings in Seismic Design," Architectural Institute of Japan, 1990.

[15] Park, Y.J., "A New Conversion Method From Response Spectrum to PSD Functions," technical note submitted for possible publication to Journal of Engineering Mechanics, ASCE, 1994.
[16] Davenport, A.G., "Note on the Distribution of the Largest Value of a Random Function with Application to Gust Loading," Proceeding of ICE, Vol. 28, June 1964, pp. 187-196.
[17] International Mathematics and Statistics Libraries, "IMSL-Library Reference Manual," Houston, Texas, 1988.
[18] U.S. Atomic Energy Commission, "Regulatory Guide 1.60," Revision 1, Dec. 1973.
[19] Wiegel, R.L., "Earthquake Engineering," Prentice-Hall, 1970, pp. 403-447.

APPENDIX. PEAK DISTRIBUTION FUNCTIONS

In most of the previous studies, the Rayleigh distribution was used in determining both the equivalent stiffness and damping, i.e., p_1 and p_2 of eqs. (7) and (8). In this study, the use of three different distribution models are recommended for p_1 and p_2, as well as for the maximum response statistics. For determining the equivalent modal damping value in eq. (8), the following Rayleigh distribution is used;

$$p_2(u,\sigma_\epsilon) = \frac{u}{\sigma_\epsilon^2} \exp\left(-\frac{u^2}{2\sigma_\epsilon^2}\right) \tag{30}$$

Whereas for the equivalent component stiffness in eq. (7), the Gumble type I distribution is used as,

$$p_1(u) = \exp\left[-\exp\left\{-\alpha_u (u - u_u)\right\}\right] \tag{31}$$

in which, the extreme distribution parameters, u_u and α_u, are determined based on the above Rayleigh distribution as,

$$F(u_u) = \int_0^{u_u} \frac{\lambda}{\sigma_\epsilon^2} \exp\left(-\frac{\lambda^2}{2\sigma_\epsilon^2}\right) d\lambda = 1 - \frac{1}{M_T} \tag{32}$$

$$\alpha_u = M_T \cdot f(u_u) = \frac{M_T\, u_u}{\sigma_\epsilon^2} \exp\left(-\frac{u_u^2}{2\sigma_\epsilon^2}\right) \tag{33}$$

in which, M_T is the equivalent mean number of peaks defined as,

$$M_T = \frac{\sigma_{\dot\epsilon}}{2\pi\, \sigma_\epsilon} \tag{34}$$

where, $\sigma_{\dot\epsilon}$ is the standard deviation of the 2nd derivative of the strain response.

For evaluating the maximum response statistics, the same Gumble type-I distribution of eq. (31) is used; in which, the parameters α_u and u_u are determined from the mean number of peaks per unit time, $N_T(u)$, as

$$T \cdot N_T(u_u) = 1.0, \quad \alpha_u = \frac{d}{du}\left\{T \cdot N_T(u)\right\}_{u = u_u} \tag{35}$$

Based on the Gaussian assumption on the response variables of the equivalent linear system, the following approximate solution is available for $N_T(u)$:

$$N(u) = \frac{\sigma_3(1 - \nu^2)}{4\pi\sigma_2}\left\{1 - erf\frac{u}{\sigma_1\sqrt{2(1-\nu^2)}}\right\} \cdot \frac{\sigma_2}{2\pi\sigma_1}\exp\left(-\frac{u^2}{2\sigma_1^2}\right) \tag{36}$$

$$\text{where, } \nu = \frac{\sigma_2^2}{\sigma_1\sigma_3},\ \sigma_1^2 = E[\epsilon^2],\ \sigma_2^2 = E\left[\dot\epsilon^2\right],\ \sigma_3^2 = E\left[\ddot\epsilon^2\right]$$

The selection of the above peak distribution functions is purely empirical and based on the past simulation studies on hysteretic systems (e.g., Refs. [5], [7] and [11]).

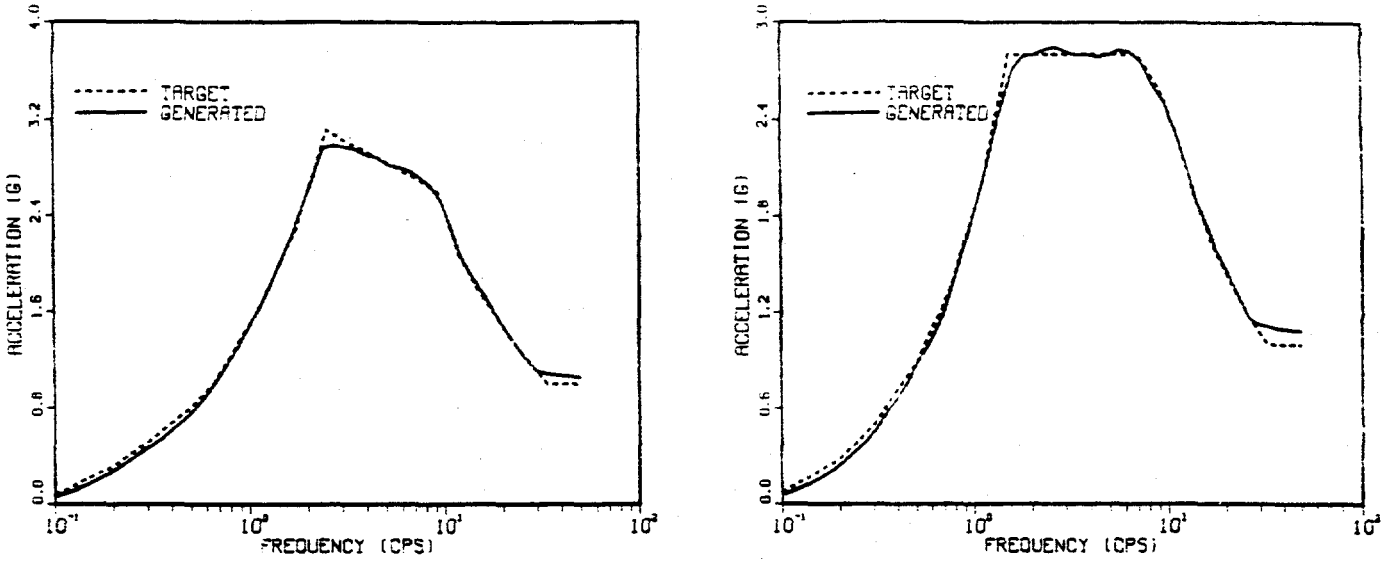

(a) REG 1.60 (b) Newmark-Hall

Fig. 1 Target and Simulated Response Spectra (for CELA)

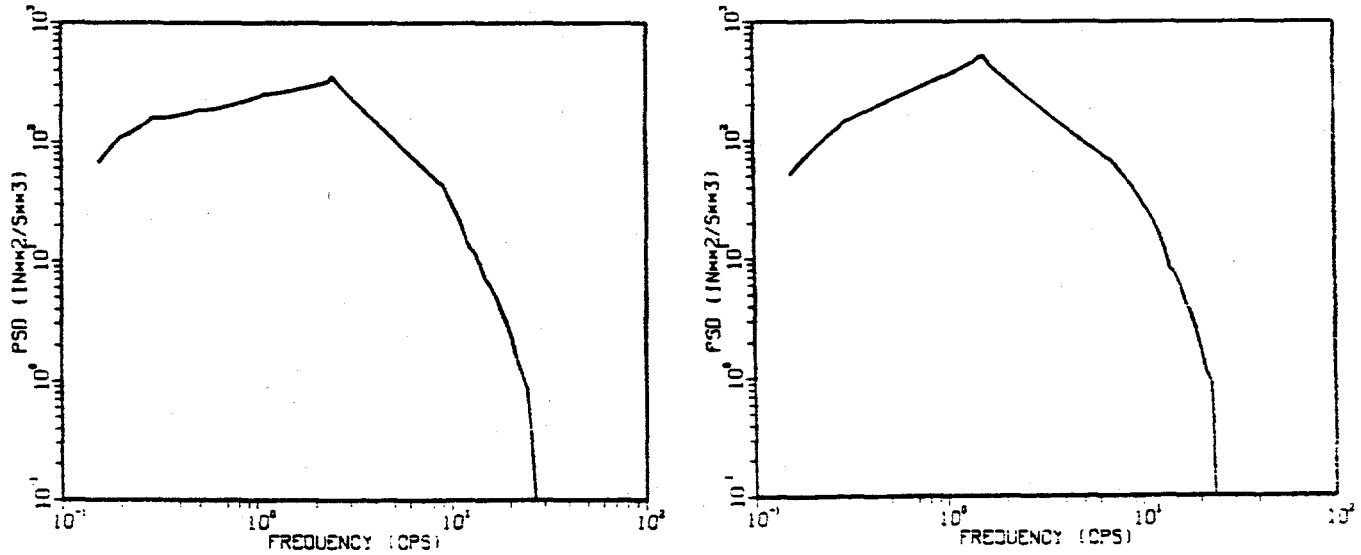

(a) REG 1.60 (b) Newmark-Hall

Fig. 2 Equivalent PSD Functions (for CELA)

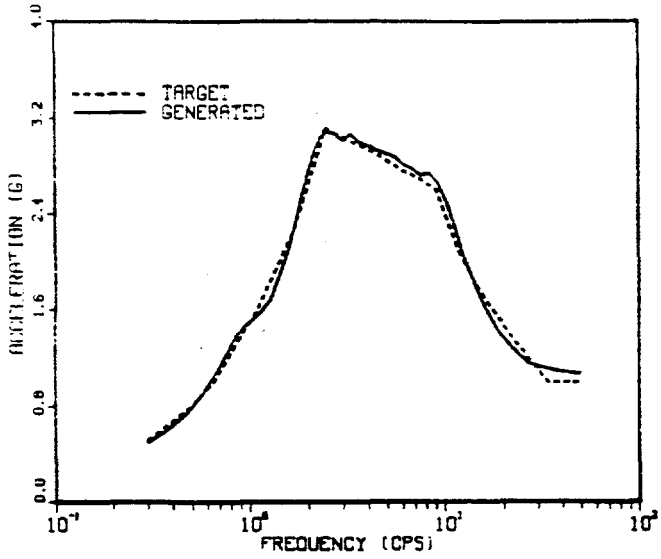

(a) REG 1.60

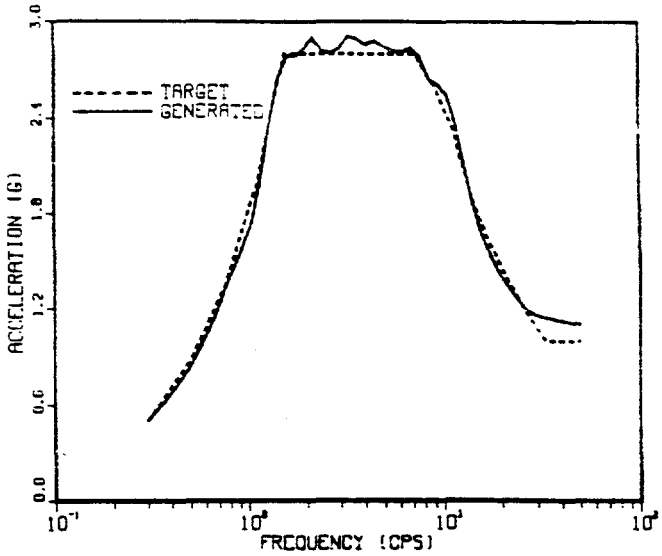

(b) Newmark-Hall

Fig. 3 Target and Simulated Response Spectra (for SELA)

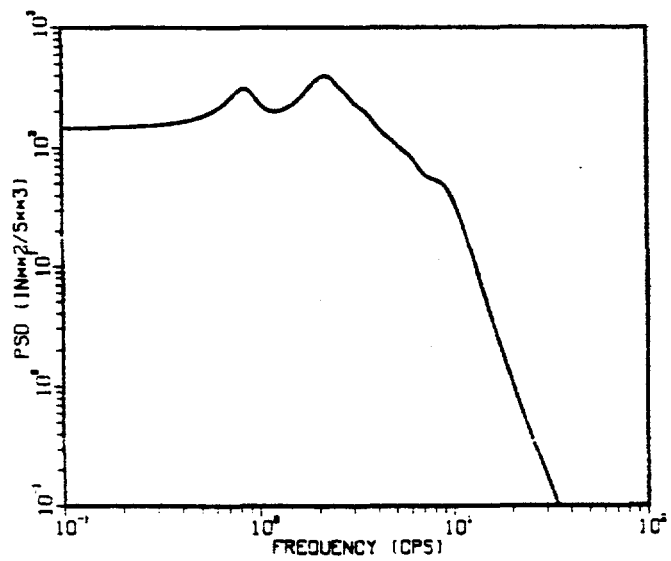

(a) REG 1.60

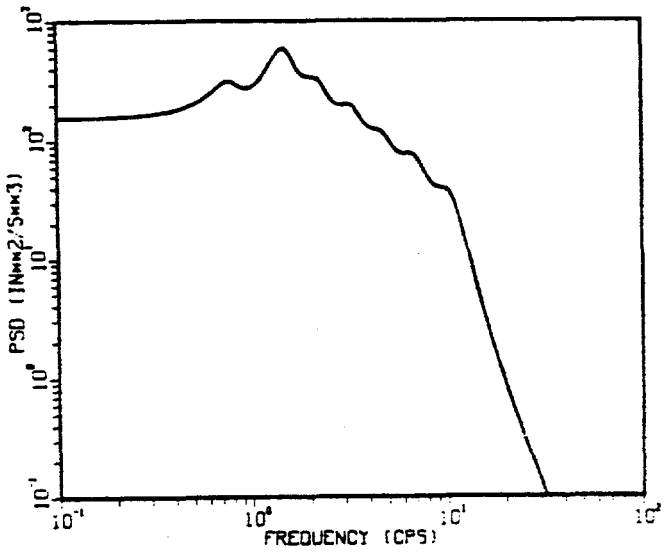

(b) Newmark-Hall

Fig. 4 Equivalent PSD Functions (for SELA)

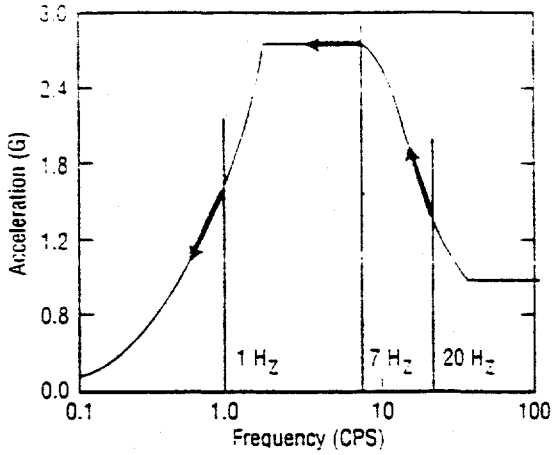

Fig. 5 Newmark-Hall Spectrum and Vibration Frequencies of SDOF

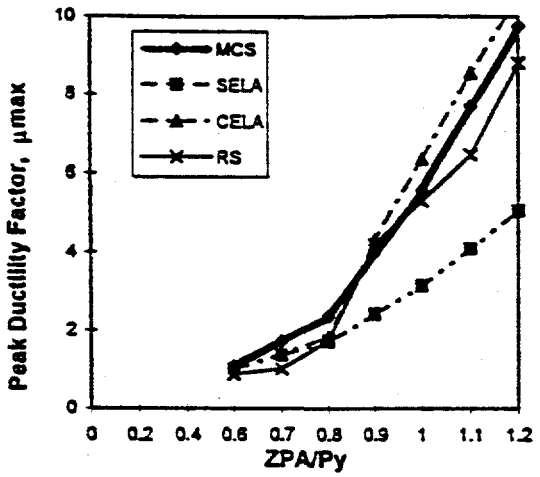

(a) Bilinear model (f = 20 Hz)

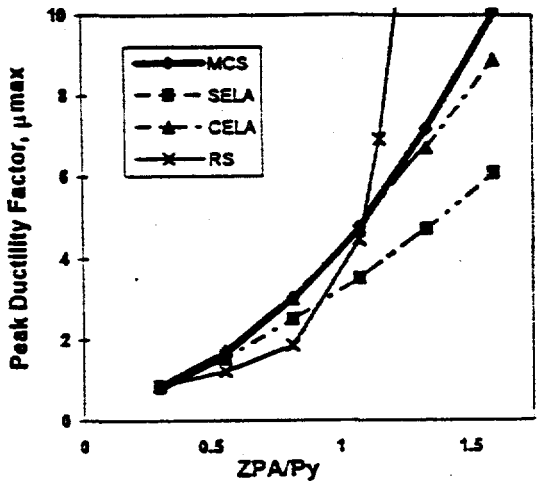

(b) Bilinear Model (f = 7 Hz)

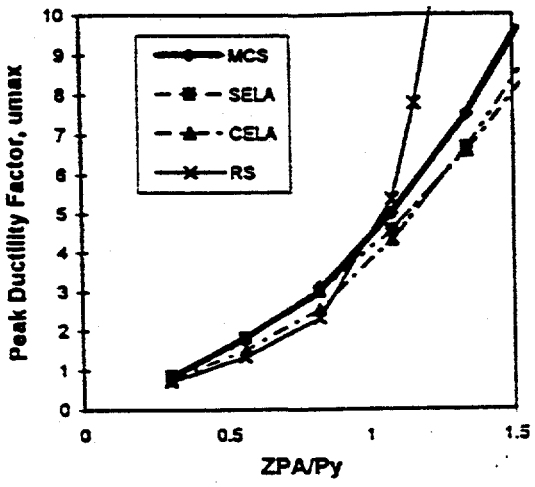

(c) Smoothed Model (f = 7 Hz)

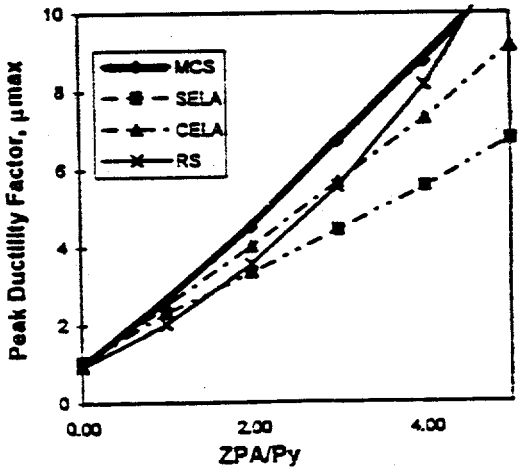

(d) Bilinear Model (f = 1 Hz)

Fig. 6 Comparisons of Nonlinear Responses

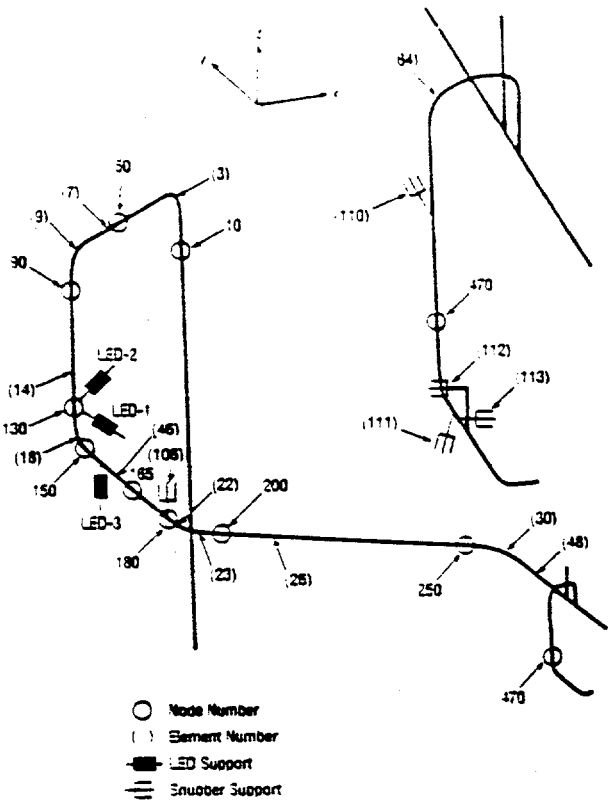

Fig. 7 F.E. Model of Main Steam Line

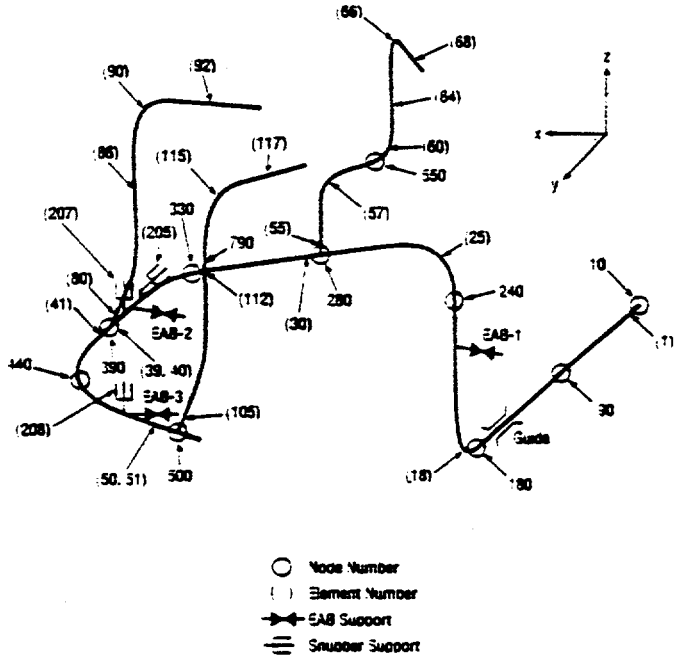

Fig. 8 F.E. Model of Feedwater Line

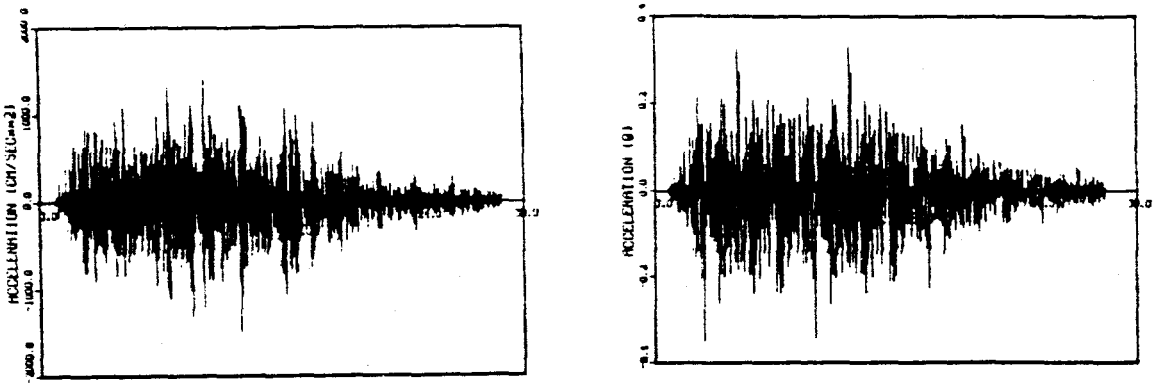

(a) Horizontal (Peak = 1.5 g) (b) Vertical (Peak = 0.35 g)

Fig. 9 Base Motions for Piping Models

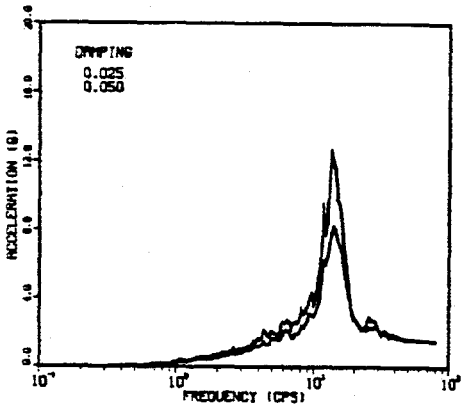

Fig. 10 Response Spectra of Horizontal Motion

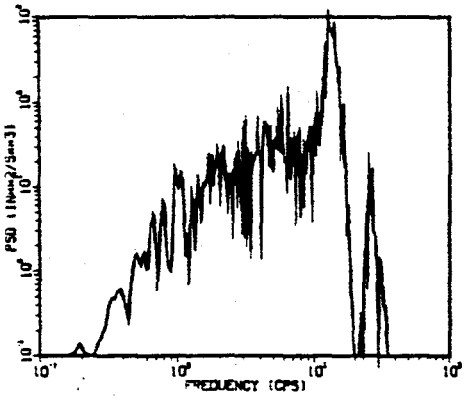

Fig. 11 Equivalent PSD Function of Horizontal Motion

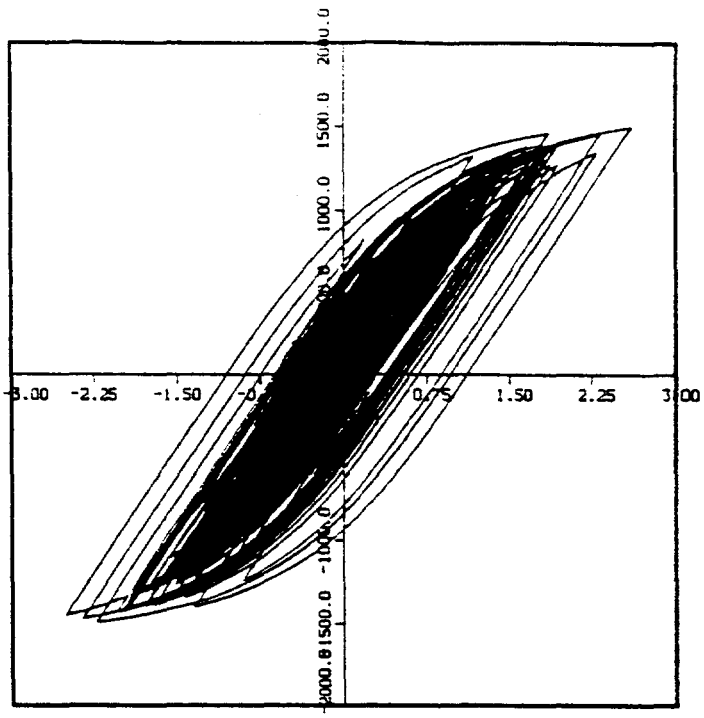

Fig. 12 Example of Hysteretic Response of E.A. Support (LED-1 of M-line)

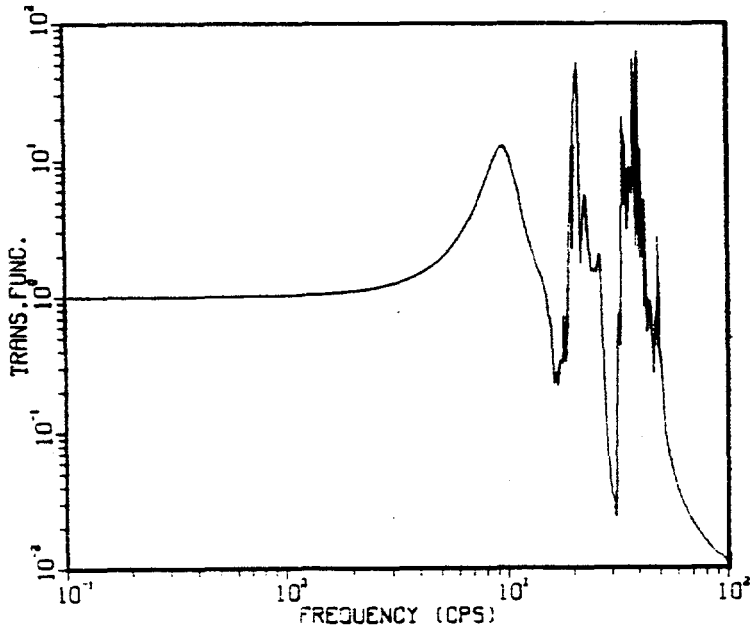

Fig. 13 Example of Acceleration Transfer Function (Node - 390 of F-line)